7B.3 A New Surface-based Polarimetric Hydrometeor Classification Algorithm for the WSR-88D Network

Terry J. Schuur[1,2], Alexander V. Ryzhkov[1,2], Heather D. Reeves[1,2], J. Krause[1,2], Matthew R. Kumjian[1,2,3], Kimberly L. Elmore[1,2], and Kiel L. Ortega[1,2]

[1]Cooperative Institute for Mesoscale Meteorological Studies, University of Oklahoma
Norman, Oklahoma

[2]NOAA/OAR/National Severe Storms Laboratory
Norman, Oklahoma

[3]Advanced Studies Program, National Center for Atmospheric Research
Boulder, Colorado

1. INTRODUCTION

The classification of cold-season precipitation at the surface is complicated by the broad range of hydrometeor types that might result from processes that occur below the height of the radar's lowest elevation sweep. For example, a shallow layer of subfreezing air near the surface might lead to either a complete refreezing of drops (ice pellets) or refreezing upon contact with the surface (freezing rain). Both of these hydrometeor types are difficult to determine using radar data alone, and may not be observed at all at distances > 50 km from the radar. Because of this, the fuzzy-logic-based hydrometeor classification algorithm that was deployed on the WSR-88D network (Park et al., 2009), which gives classifications on conical surfaces, often provides results in transitional winter weather events that are not at all representative of the precipitation type observed at ground level.

In this paper, we describe the continued development of a new polarimetric Winter surface Hydrometeor Classification Algorithm (WsHCA) that uses thermodynamic output from numerical models to provide a surface-based classification. In short, the introduction of thermodynamic output from numerical models provides an opportunity to not only enhance classification in regions where radar data are available, but also to extend classification capabilities to more distant ranges where low-level radar data are not available.

Corresponding author address: Terry J. Schuur
University of Oklahoma/CIMMS
National Weather Center
120 David L. Boren Blvd., Norman, OK, 73072
E-mail: schuur@ou.edu

2. ALGORITHM DEVELOPMENT

The continued development of the WsHCA follows the work first reported by Schuur et al. (2012), in which profiles of T_W derived from the Rapid Update Cycle (RUC) model are used to develop a "background classification" that is later accepted or rejected based on polarimetric radar observations. As described in Schuur et al., four different profiles of T_W are identified (see Fig. 1) where H_0, H_1, and H_2 in Fig. 1 depict the heights of the 0°C crossing points in the profiles. Making use of the studies by Czys et al. (1996), Zerr (1997), and Rauber et al. (2001), the T_W profiles are then used to create a background classification that consists of six precipitation categories: 1) snow (SN), 2) wet snow (WS), 3) freezing rain (FR), 4) ice pellets (IP), 5) a combination of freezing rain and ice pellets (FR/IP), and 6) rain (RA). In this procedure, the threshold for the maximum and minimum acceptable T_W profiles in the warm (T_{Wmax}) and cold (T_{Wmin}) layers, respectively, are derived from a visual inspection of the scatterplots presented by Figs. 5 and 6 of Zerr (1997).

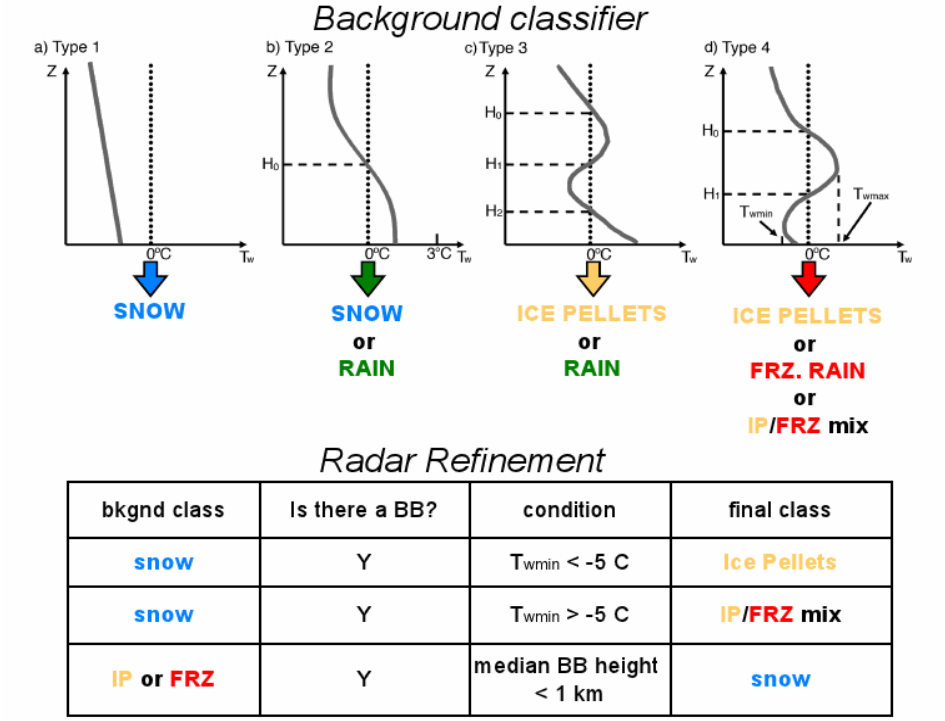

Radar Refinement

bkgnd class	Is there a BB?	condition	final class
snow	Y	T_{wmin} < -5 C	Ice Pellets
snow	Y	T_{wmin} > -5 C	IP/FRZ mix
IP or FRZ	Y	median BB height < 1 km	snow

Fig. 1. Fig. 4: Four types of vertical profiles of wet-bulb temperature (T_W) corresponding to four or more types of precipitation and table showing simplified criteria, based on the radar determination of an elevated warm layer/bright band, used for the modification of the background classification.

- When $T_{Ws} \geq 3°C$, the precipitation at the surface is classified as RA.
- For profile Type 1 (Fig. 1a) where $T_W < 0°C$ throughout the entire depth of the profile, the surface precipitation is classified as SN.
- For profile Type 2 (Fig. 1b), where $0° < T_{Ws} < 3°C$ and the T_W profile crosses the 0°C level one time, the precipitation at the surface is classified as WS if $H_0 < 1$ km. Otherwise, the precipitation at the surface is classified as RA.
- For profile Type 3 (Fig. 1c), where $0° < T_{Ws} < 3°C$ and the T_W profile crosses the 0°C level three times, the precipitation at the surface is classified as IP if $0°C \leq T_{Wmax} < 2°C$ and $T_{Wmin} < -5°C$, where T_{Wmax} is the maximum T_W in the vertical profile and T_{Wmin} is the minimum T_W in the vertical profile. Otherwise the precipitation is classified as RA.
- For profile Type 4 (Fig. 1d), where $T_{Ws} < 0°C$ and the T_W profile crosses the 0°C level two times, the precipitation at the surface is classified as FR if $T_{Wmax} > 2°C$ and $T_{Wmin} \geq -5°C$ and IP if $T_{Wmax} < 2°C$ and $T_{Wmin} < -5°C$. Otherwise the precipitation at the surface is classified as FR/IP.

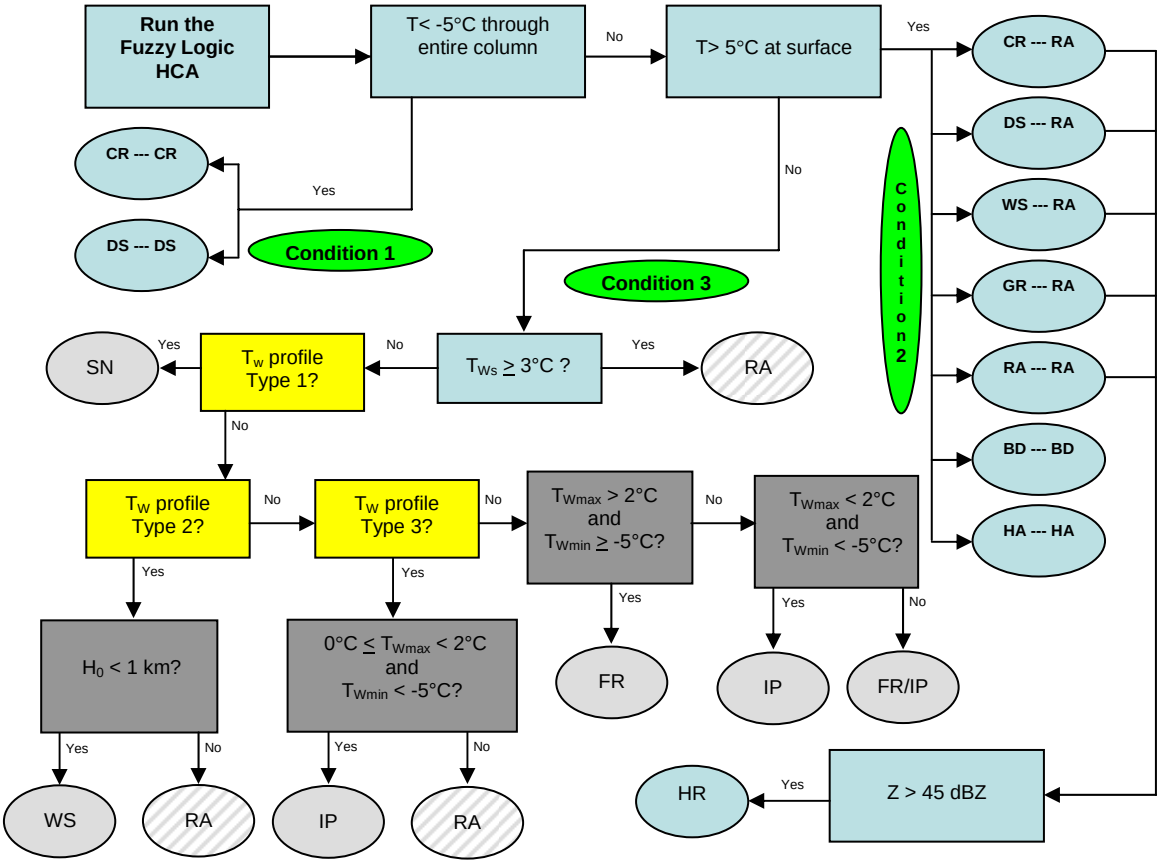

Fig. 2. Modified flow chart (compare to Fig. 4 of Schuur et al. 2012) showing logic for the determination of precipitation types. Algorithm starts by running fuzzy-logic-based HCA. Fuzzy-logic-based classifications from lowest elevation sweep are projected to the surface as snow or ice crystals for cold season events where the entire atmospheric column above a location has T < -5ºC (condition 1) and as rain, big drops, or hail for warm season events where the surface temperature at a location is > 5ºC (condition 2). Full model-based background classification scheme is implemented for intermediate conditions typical of transitional winter weather events (condition 3). Corresponding T_W profile types are shown in Fig. 1.

Polarimetric radar data are then inspected to either confirm or reject the background classification. For example, if the polarimetric radar data provides clear evidence of a melting layer in a region that had a background classification of dry snow, the background classification is found to be inconsistent with the radar observations and the surface classification is reassigned based on a set of empirical rules. Those rules are described in detail by Schuur et al. (2012) and summarized in the table in Fig. 1.

In the past 2 years, the algorithm has undergone numerous enhancements. First, it has been modified to use the higher resolution output provided by the High-Resolution Rapid Refresh (HRRR) model. The HRRR analyses are produced every hour by assimilating observed variables into the 1-hr forecast from the previous cycle using a variational three-dimensional analysis scheme. The output are then mapped to a radar-centric coordinate system, thereby providing better resolution and improved diagnostic capabilities over

that previously available from the RUC. Second, recognizing that the background classification is only necessary for the narrow range of atmospheric temperature profiles typical of transitional winter events, the algorithm has been modified to include precipitation type designations (made on conical surfaces) from the fuzzy-logic-based scheme of Park et al. (2009). The goal with the development of the WsHCA has never been to create an algorithm to replace the fuzzy-logic-based HCA but to develop a surface-based algorithm that would complement it. Therefore, combining the surface-based algorithm with the fuzzy-logic-based HCA not only creates a single algorithm that can be used to provide precipitation type classification at *both* the surface and aloft, but also results in an algorithm that is able to provide surface hydrometeor type designations for both cold- and warm-season precipitation systems. To accomplish this, fuzzy-logic classifications from the lowest elevation sweep are projected to the surface as snow or ice crystals for "cold season" conditions where the entire atmospheric column above a location has T < -5ºC and as rain, big drops, or hail for "warm season" conditions where the surface temperature at a location is > 5ºC. For intermediate conditions typical of transitional winter weather events, the algorithm continues to use, as before, vertical profiles of T_W to provide the background precipitation classification type. As with the earlier version of the WsHCA, polarimetric radar observations are then used to either confirm or reject the background classification for transitional winter weather. A separate hail sizing plug-in being developed for warm-season precipitation (Ortega et al., 2013) will provide added value by classifying hail into 3 distinct size categories: hail, large hail, and giant hail. A flow chart describing this classification process is presented by Fig. 2.

Finally, in order to fine tune the algorithm, a team of researchers with a wide range of expertise has been assembled to identify and improve shortcomings in every component of the existing algorithms classification capabilities. This includes optimizing the fuzzy logic weighting functions, improving bright band determination (Krause et al. 2013), evaluating the performance of model-based background classification schemes (Reeves et al. 2013). All of these efforts are ongoing and are reported on by separate papers at this conference.

3. CASE STUDY: KPBZ ON 21 JANUARY 2012

A transitional winter weather event sampled by the Pittsburgh, PA (KPBZ) radar on 21 January 2012 is presented here to illustrate the algorithm's performance. In particular, this event highlights a common problem with the fuzzy-logic-based precipitation classification algorithm, that is, the importance of an accurate determination of the melting layer height to the classification process. Fig. 3 presents 0.5° elevation reflectivity (Z_H), differential reflectivity (Z_{DR}), and correlation coefficient (ρ_{HV}) from the KPBZ radar at 080332 UTC and melting layer height (H0, refer to Fig. 1) from the HRRR analyses at 08 UTC on 21 January 2012. The bright band detection algorithm (Giangrande et al., 2008) currently deployed on the WSR-88D network relies on bright band detections made between 4 and 10° elevations. The top and bottom bright band heights detected at these elevations are then projected outward along each azimuth to obtain the corresponding ranges that those heights would be detected at the 0.5° elevation scan. This technique, of course, makes the unrealistic assumption that the height of the elevated warm layer is constant along any given azimuth. Another complication arises if the warm layer is not deep enough into the radar domain to be sampled by the 4-10° elevation sweeps. In that case, the algorithm does not detect a bright band at all (even though it may be apparent at more distant ranges on lower elevation scans) and reverts to using the melting layer height above the radar location, as determined from either the latest sounding or model run, across the entire radar domain.

It is clear from the polarimetric variables in Fig. 3 that transitional winter weather is occurring just to the south of KPBZ. To the north of KPBZ, a uniform field of Z_{DR} ~ 0.3 dB and ρ_{HV} > 0.98 is consistent with a widespread region of dry snow. This is supported by the H0 (melting layer height)

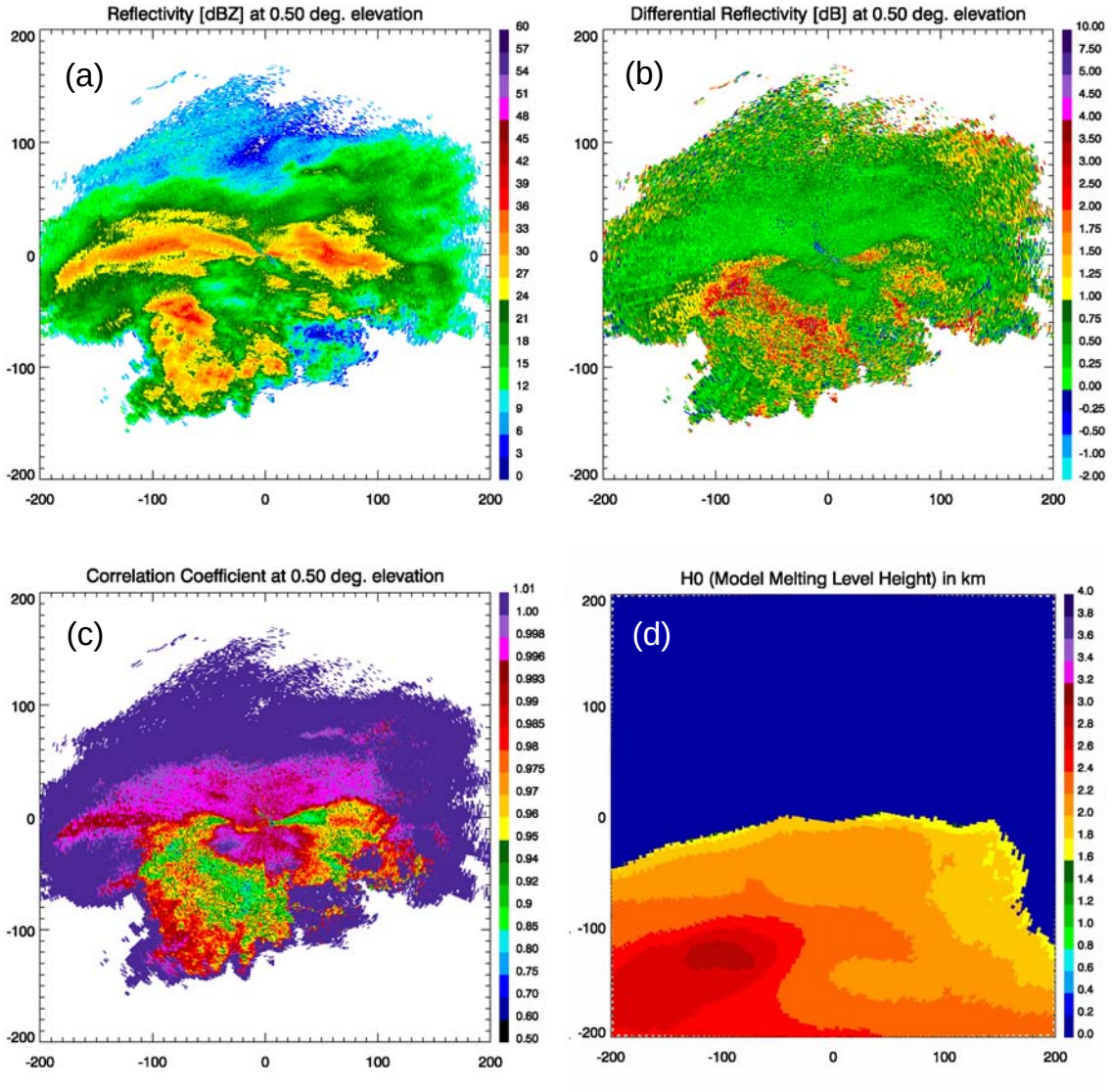

Fig. 3. PPIs of (a) Radar reflectivity (Z_H), (b) differential reflectivity (Z_{DR}), correlation coefficient (ρ_{HV}) at 0.5° elevation from the Pittsburgh, PA KPBZ radar at 080332 UTC and (d) H0 (melting level height) from the HRRR model at 08 UTC on 21 January 2012.

field in Fig. 3, which shows an elevated warm layer covering much of the domain to the south of KPBZ, but not quite reaching KPBZ itself, which appears to be embedded in the deep, cold air mass (consistent with the polarimetric indication of widespread dry snow). This is further illustrated by Fig. 4, which depicts reconstructed vertical cross sections of KPBZ Z_H, Z_{DR}, and ρ_{HV} and T_W from the HRRR model (all panels with T_W contours overlaid) along the 180° azimuth at 08 UTC. The T_W cross section in Fig. 4 indicates that the elevated warm layer extends northward to a location ~ 8 km south of the KPBZ radar. This too is in good agreement with the polarimetric variables, which provide clear evidence of an elevated bright band signature (enhanced Z and Z_{DR} and reduced ρ_{HV}) that dips to ground just to the south of the radar at a location close in proximity to where the model-indicated warm layer ends.

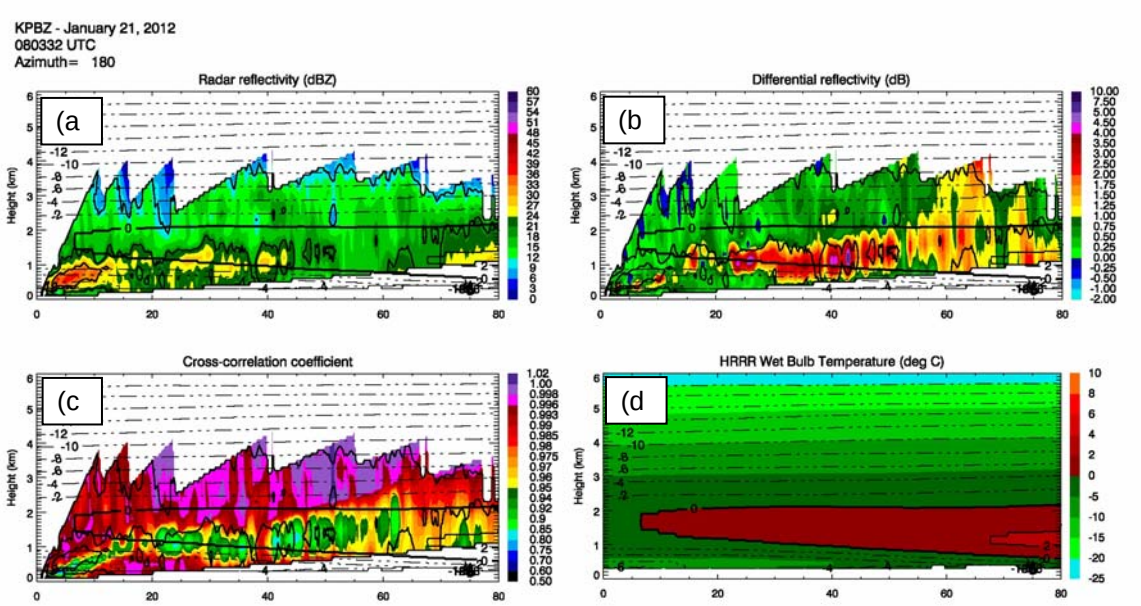

Fig. 4. Reconstructed vertical cross sections of (a) Radar reflectivity (Z_H), (b) differential reflectivity (Z_{DR}), correlation coefficient (ρ_{HV}) at 180° azimuth from the Pittsburgh, PA KPBZ radar at 080332 UTC and (d) T_W from the HRRR model at 08 UTC on 21 January 2012. T_W contours are also overlaid on the polarimetric variables.

An examination of the radar fields and model output from 01 UTC through 17 UTC (not shown) indicates that the elevated warm layer was located well to the south-southwest of the radar early in the time period, advanced northward and reached its northernmost extent at approximately 07 UTC, and then slowly retreated back to the south as the cold air mass from the north overtook it later in the time period. Over the course of the entire event, KPBZ was located under the elevated warm layer for approximately 1 hour; at other times, KPBZ was embedded within the deep, cold air mass to the north where temperatures were subfreezing through the entire atmospheric column. More importantly, for most of the event, the elevated warm layer, though covering much of the domain to the south of the radar, was located too far from KPBZ to be detected by the 4-10° elevation scans used by the bright band detection algorithm. This means that the fuzzy-logic-based HCA would have used a bright band height (determined from either sounding or model) of 0.0 km across the entire domain. Furthermore, the elevated warm layer was located too far from the radar for any precipitation processes (such as full or partial refreezing) that might be occurring underneath it to be sampled by the 0.5° elevation sweep. In fact, Fig. 5, which shows HRRR surface T_W at 08 UTC, can be compared to the H0 field in Fig. 3 to see that T_W at the surface was < 0°C under much of the elevated warm layer at 08 UTC, suggesting that ice pellets and/or freezing rain were indeed a possibility in this region.

Fig. 6 shows the fuzzy-logic-based HCA and final WsHCA products for this event at 08 UTC while Fig. 7 shows the conditions, or paths followed on the flow chart in Fig. 2 for each surface-based designation in the final product at 08 UTC. A comparison of panels Fig. 6a and 6b shows the dramatic difference in the surface classification from the two algorithms. As noted earlier, since the radar was unable to get a sufficient number of bright band detections at 4-10° elevations and was, furthermore, embedded within the deep, cold air mass, a default model bright band height of 0.0 km was used, resulting in a classification of dry snow and ice crystals over most of the radar domain. On the other hand, the WsHCA

provides a much more realistic classification of surface-based hydrometeor types to the south of the KPBZ, where much of the domain is covered by an elevated warm layer (Fig. 3d) that is sometimes located over subfreezing surface temperatures (cf. Fig. 5). Precipitation types classified in this region to the south of KPBZ include rain, freezing rain, ice pellets, an ice pellet / freezing rain mix, and wet snow.

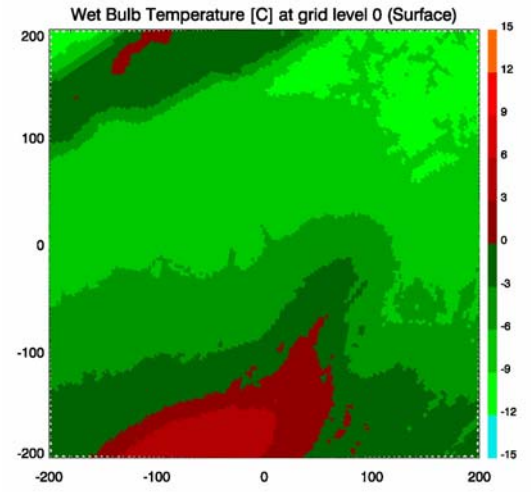

Fig. 5. Surface T_W from the HRRR model at 08 UTC on 21 January 2012.

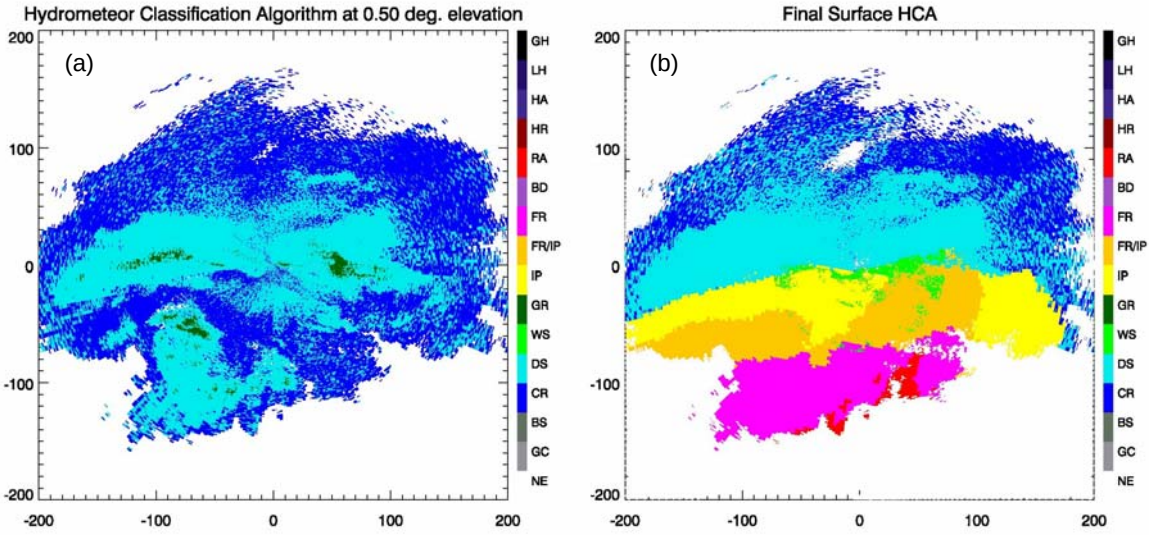

Fig. 6. Precipitation type classification centered on the KPBZ radar from the (a) fuzzy-logic-based HCA at 0.5 elevation, and (b) WsHCA at 08 UTC on 21 January 2012. Precipitation type categories are no echo (NE), ground clutter (GC), biological scatterers (BS), crystals (CR), dry snow (DS), wet snow (WS), graupel (GR), ice pellets (IP), freezing rain/ice pellets (FR/IP), freezing rain (FR), big drops (BD), rain (RA), heavy rain (HR), hail (HA), large hail (LH), and giant hail (GH).

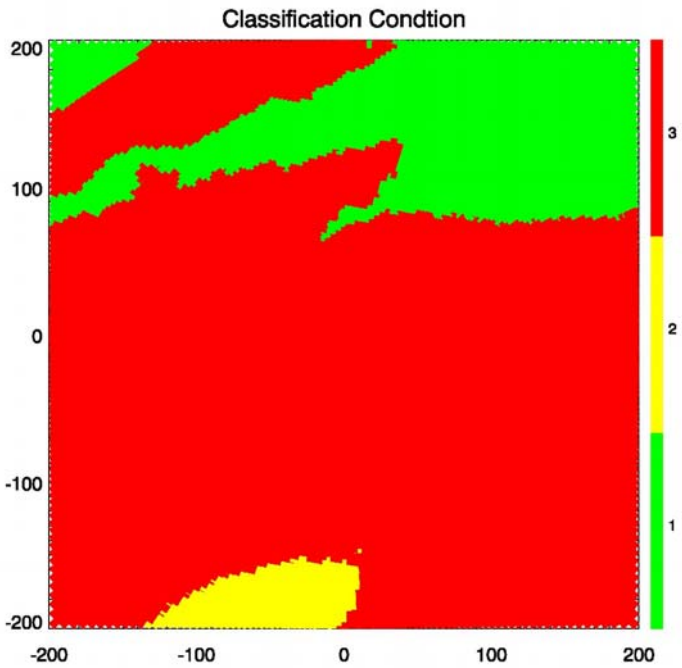

Fig. 7. Classification condition followed in the decision tree in Fig. 2 centered on the KPBZ radar at 08 UTC on 21 January 2012. Condition 1 (green) shows locations where snow and ice crystals are projected to the surface for "cold season" conditions when the entire atmospheric column above that location has T < -5ºC, condition 2 (yellow) shows locations where all ice categories are projected to the surface as either rain, big drops, or hail for "warm season" conditions when the surface temperature at a location is > 5ºC, and condition 3 (red) shows locations where intermediate conditions typical of transitional winter weather are met and the full WsHCA is run to determine surface precipitation type.

4. SUMMARY AND CONCLUSIONS

Accurate surface-based classification of hydrometeor type in transitional winter weather events is often difficult due to the broad range of cold-season hydrometeor types that are possible from processes that occur below the height of the radar's lowest elevation sweep. The new Winter surface Hydrometeor Classification Algorithm (WsHCA) described in this paper is therefore being developed to use thermodynamic information from numerical models to not only enhance classification capabilities in regions where radar data are available, but to also extend classification to more distant ranges where low-level radar data are not available. Vertical profiles of T_W are used develop a model-based background classification that is later modified, if necessary, but polarimetric radar observations. The algorithm has been improved from previous reported versions by using higher resolution model output from the HRRR model and combined with the fuzzy-logic-based HCA of Park et al. (2009) to provide a "hybrid" algorithm that provides precipitation type classifications both at the surface and aloft. Logic added to the algorithm to project fuzzy-logic classifications from the lowest elevation sweep to the surface as snow or ice crystals for "cold season" conditions where the entire atmospheric column above a location has T < -5ºC and as rain, big drops, or hail for "warm season" conditions where the surface temperature at a location is > 5ºC allows the algorithm to be used for a wider range (both cold-and warm-season) of precipitation events. For intermediate conditions typical of transitional winter weather, the algorithm continues to use vertical profiles of T_W to provide the background precipitation classification type. A team of researchers

with a broad range of expertise has also been assembled to identify and improve all aspects of the algorithm performance, including the optimization of fuzzy weighting functions, bright band determination, and model-based background classifications.

Initial testing of the algorithm has demonstrated it's effectiveness at classifying transitional winter weather precipitation types, such as ice pellets and freezing rain, in regions where the fuzzy-logic-based HCA has trouble determining melting layer height, erroneously uses a single bright band height over the entire radar domain, and then mistakenly provides a classification of dry snow in regions where the presence of an elevated warm layer (as indicated by the HRRR output) would prohibit such a classification. Future work on this algorithm will include an extensive effort to improve the algorithm performance by validating the algorithm results against surface precipitation type observations obtained from the mobile Precipitation Identification Near the Ground (mPING, Elmore et al., 2013) project. The mPING project (http://www.nssl.noaa.gov/projects/ping/display/), which was developed as part of the team effort to develop a surface-based precipitation classification algorithm, collects time-stamped and geo-tagged precipitation reports from the general public using a mobile phone app. To date, well in excess of 100,000 reports have been collected in winter weather events.

5. ACKNOWLEDGEMENTS

Funding was provided by NOAA/Office of Oceanic and Atmospheric Research under NOAA-University of Oklahoma Cooperative Agreement #NA11OAR4320072, U.S. Department of Commerce, and by the U.S. National Weather Service, Federal Aviation Administration, and Department of Defense program for modernization of NEXRAD radars.

6. REFERENCES

Czys, R., R. Scott, K. Tang, R. Przybylinski, and M. Sabones, 1996: A physically based nondimensional parameter for discriminating between locations of freezing rain and sleet. *Wea. Forecasting*, **11**, 591-598.

Elmore, K. L., Z. L. Flamig, V. Lakshmanan, B. T. Kaney, V. Farmer and L. P. Rothfusz, 2013: mPING: Crowd-sourcing weather reports for research. Bull. Amer. Meteor. Soc., In review.

Giangrande, S. E., J. M. Krause, and A. V. Ryzhkov, 2008: Automated designation of the melting layer with a polarimetric prototype of the WSR-88D radar. *J. Appl. Meteor. Climatol.,* **47**, 1354-1364.

Krause, J., V. Lakshmanan, and A. Ryzhkov, 2013: Improving detection of the melting layer in the dual-polarimetric radar volume using model data and object identification techniques. *36th Conference on Radar Meteorology*, Breckenridge, CO, American Meteorological Society, Boston, 262.

Ortega, K. L., A. V. Ryzhkov, J. Krause, P. Zhang, and M. R. Kumjian, 2013: Evaluating a Hail Size Discrimination Algorithm for dual-polarized WSR-88Ds using high-resolution reports and forecaster feedback. *36th Conference on Radar Meteorology*, Breckenridge, CO, American Meteorological Society, Boston, 7B.4.

Park, H.-S., A. V. Ryzhkov, D. S. Zrnic, and K-.E. Kim, 2009: The hydrometeor classification algorithm for the polarimetric WSR-88D: Description and application to an MCS. *Wea. Forecasting*. **24**, 730-748.

Rauber, R. M., L. S. Olthoff, M. K. Ramamurthy, and K. E. Kunkel, 2001: Further investigations of a physically based, nondimensional parameter for discriminating between locations of freezing rain and ice pellets. *Wea. Forecasting*, **16**, 185-191.

Reeves, H. D., T. J. Schuur, A. V. Ryzhkov, K. L. Elmore, J. Krause, and K. L. Ortega, 2013: Testing of a background classification algorithm for use with dual-polarized radars in determining precipitation type at the surface. *36th Conference on Radar Meteorology*, Breckenridge, CO, American Meteorological Society, Boston, 318.

Schuur, T. J., Park, H.- S., A. V. Ryzhkov, and H. D. Reeves, 2012: Classification of precipitation types during transitional winter weather using the RUC model and polarimetric radar retrievals. *J. Appl. Meteor. Climate*, **51**, 763-779. DOI: 10.1175/JAMC-D-11-091.1.

Zerr, R. 1997: Freezing rain, an observational and theoretical study. *J. Appl. Meteor.,* **36**, 1647-1661.